

Minimum Time vs Maximum Exit Velocity Path Optimization During Cornering

E. Velenis* and P. Tsiotras*

*Georgia Institute of Technology

School of Aerospace Engineering, Atlanta, GA, USA

{efstathios.velenis, p.tsiotras}@ae.gatech.edu

Abstract—Numerical optimization has been used as an extension of vehicle dynamics simulation in order to reproduce trajectories and driving techniques used by expert race drivers and investigate the effects of several vehicle parameters in the stability limit operation of the vehicle. In this work we investigate how different race-driving techniques may be reproduced by considering different optimization cost functions. We introduce a bicycle model with suspension dynamics and study the role of the longitudinal load transfer in limit vehicle operation, i.e., when the tires operate at the adhesion limit. Finally we demonstrate that for certain vehicle configurations the optimal trajectory may include large slip angles (drifting), which matches the techniques used by rally-race drivers.

I. INTRODUCTION

Modelling for simulation and control of automotive systems has been a subject of intense research in the literature [1], [2], [3]. This research has led to several methodologies for simulating vehicle dynamics in order to evaluate the performance of vehicles, develop new systems to enhance safety and performance, as well as to automate several tasks during driving.

Expert race-car drivers operate the vehicles at the limits of their stability envelope, which makes the role of the different vehicle parameters involved extremely difficult to investigate solely by means of numerical simulation. To this end, numerical optimization techniques have been used in the literature in order to reproduce trajectories and driving techniques similar to those of expert race car drivers. In [4] the numerical solution of the *optimal time* problem for a car driving through a segment of the Suzuka F1 circuit has been presented. An accurate 3D description of the road is used which even includes bank. The car model used is over-simplified however, as the vehicle is regarded as a particle. Another approach for the numerical optimization problem is presented in [5]. The constraint of the road is included as an additional term in the cost function, while a comprehensive 4-wheel car model, including nonlinear tire friction, load transfer, aerodynamic forces and driveline constraints is used. In [6] the authors have solved a similar optimization problem as in [5] using an equally rich car model and a more efficient optimization algorithm. In addition, the role of yaw inertia was studied in that reference. In [7] the authors presented the optimal time solution for the Suzuka and Barcelona F1 circuits and studied the influence of vehicle mass to the optimal trajectory.

A common factor of all the work in the literature to

date is that race driving is assumed to be equivalent to driving in minimum time through the whole path. This is true in cases such as F1 time trials, where drivers have driven through the whole circuit several times before the final race, trying to optimize their path in order to achieve the best overall lap time. Similarly, in rally racing the driver again has to follow a path in minimum time. However, in off-terrain rally-races extensive trials do not necessarily take place, and the driver is expected to react in unpredictable and changing environments during the actual race. This is in contrast to the controlled environment of F1 circuit races. Rally-race drivers typically drive through trajectories that will allow them to react faster to any unpredictable hazard or road formation. For instance, tight corners are typically negotiated in such a way that the car is already aligned to the following road segment well before the exit of the corner, thus allowing the driver to plan ahead sooner. This often means that the driver induces drifting. In case when a straight path follows the corner, the driver is able to fully accelerate the car while still in the corner, thus maximizing the velocity at the exit of the corner.

In this work we reproduce several race-driving behaviors by considering several cases of cost functions in the numerical optimization scheme. In the following we introduce a half-car (bicycle) model with suspension dynamics. The problem of driving through a 90 deg corner is formulated as a problem in optimal control. We consider two cases for the optimization cost. In the first case we minimize time of travel (in accordance to the literature), and in the second we maximize the velocity of the car at the exit of the corner. Each scenario is calculated twice, with and without suspension dynamics in order to analyze the effects of the dynamic longitudinal normal load transfer. Finally we present a maneuver with maximum exit velocity from a corner with a different vehicle configuration, using reduced lateral tire friction and weight balance of a neutral-steering vehicle. The optimal solution includes large slip angles which resembles the way rally-race drivers perform.

II. DYNAMICS OF A HALF-CAR MODEL

In this work vehicle dynamics are modelled using the typical assumptions for a half-car model [1], [2], [3]. Non-linear tire characteristics are taken into consideration by the use of Pacejka's "Magic Formula" tire model [8]. Suspension dynamics are typically neglected in the

literature, especially when F1 cars with stiff suspensions are considered [6], [7]. In commercial passenger vehicles and especially off-road vehicles “softer” suspensions are used for passenger comfort and chassis longevity. In this paper we include the dynamics of the suspension system in our vehicle modelling, which allows a more realistic expression for the longitudinal normal load transfer compared to the approximation in [6], [7]. Most importantly, it allows us to investigate the role of the suspension parameters in limit operation of the vehicle.

A. Equations of Motion

The equations of motion of the half-car model, shown in Fig. 1, are given below.

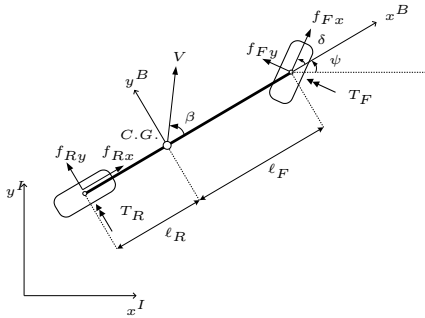


Fig. 1. Bicycle Model

$$\begin{aligned} m\ddot{x} &= f_{Fx} \cos(\psi + \delta) - f_{Fy} \sin(\psi + \delta) \\ &+ f_{Rx} \cos \psi - f_{Ry} \sin \psi \end{aligned} \quad (1)$$

$$\begin{aligned} m\ddot{y} &= f_{Fx} \sin(\psi + \delta) + f_{Fy} \cos(\psi + \delta) \\ &+ f_{Rx} \sin \psi + f_{Ry} \cos \psi \end{aligned} \quad (2)$$

$$I_z \ddot{\psi} = (f_{Fy} \cos \delta + f_{Fx} \sin \delta) \ell_F - f_{Ry} \ell_R \quad (3)$$

$$I_i \dot{\omega}_i = T_i - f_{ix} r \quad (i = F, R). \quad (4)$$

In the above equations m is the vehicle’s mass, I_z is the polar moment of inertia of the vehicle, I_i ($i = F, R$) are the moments of inertia of the front and rear wheels about the axis of rotation respectively, r is the radius of each wheel, and x and y are the cartesian coordinates of the C.G. in the inertial frame of reference. ψ is the yaw angle of the vehicle and ω_i ($i = F, R$) is the angular rate of the front and rear wheel respectively. By f_{ji} ($j = x, y, i = F, R$) we denote the longitudinal and lateral friction of the front and rear wheels, respectively. In this model the inputs are the driving/braking torques T_F and T_R at the front and rear wheels respectively, and δ is the steering angle of the front wheel. Engine, transmission and brake dynamics have been neglected. We have assumed that the longitudinal control inputs of the vehicle are the two independent torques on each wheel. However, in reality the control inputs for an automobile is the acceleration pedal and the brake pedal. Thus, the input torques of each wheel are coupled. On the other hand, several race driving techniques, such as “hand-brake cornering” (braking of the rear axle only) and “left foot braking” (simultaneous use of brakes and gas pedal varying the torque balance between front and rear axles),

do allow some independence on the longitudinal control of each axle [9].

B. Tire Friction

Tire friction forces are calculated using Pacejka’s “Magic Formula” model. This is a static, slip-based, tire friction model for combined longitudinal and lateral motion of the tire [8]. The friction forces in this model are calculated as follows. First, we define the “total slip” of the wheel as follows

$$s_i = \sqrt{s_{ix}^2 + s_{iy}^2} \quad (i = F, R), \quad (5)$$

where s_{ix} is the longitudinal and s_{iy} is the lateral slip of the i wheel. We then calculate the friction force for the “total slip” using the “Magic Formula”

$$F_i = F_{iz} D \sin(\text{Catan}(B s_i)) \quad (i = F, R). \quad (6)$$

Finally, the longitudinal and lateral friction forces are given by

$$f_{ij} = c_j \frac{s_{ij}}{s_i} F_i \quad (i = F, R \text{ and } j = x, y), \quad (7)$$

where the factor c_j is incorporated in cases of tires with different friction limits along the longitudinal and lateral directions. In case $c_x = c_y = 1$ the total tire friction force lies within a circle in the $f_{ix} - f_{iy}$ plane, while for $c_x \neq c_y$ the force lies within an ellipse.

The self-aligning torque M_z is neglected, as it is typically done in the literature [5], [6], [7].

C. Suspension Dynamics

Let z be the vertical displacement of the center of gravity of the vehicle and θ the pitch angle of the suspended mass as in Fig. 2. The dynamics of the vertical

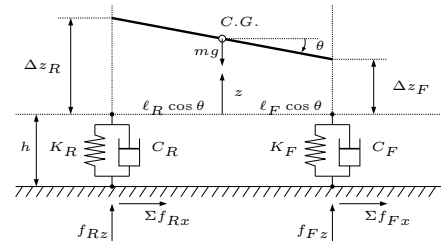


Fig. 2. Suspension Dynamics

and pitching motion of the suspended mass are described by the following equations.

$$m\ddot{z} = f_{Fz} + f_{Rz} - mg \quad (8)$$

$$\begin{aligned} I_y \ddot{\theta} &= f_{Rz} \ell_R \cos \theta - f_{Fz} \ell_F \cos \theta \\ &- \Sigma f_{Rx} (h + z) - \Sigma f_{Fx} (h + z), \end{aligned} \quad (9)$$

where, I_y is the moment of inertia of the vehicle about the center of gravity and the y body axis. By h we denote the vertical distance of the C.G. from the ground in an equilibrium state where $z = 0$. By f_{iz} ($i = F, R$) we denote the normal load forces at the front and rear axle respectively and by Σf_{ix} ($i = F, R$) we denote the

projection of the total friction force of each wheel on the x longitudinal body axis. In addition,

$$\Sigma f_{Rx} = f_{Rx} \quad \text{and} \quad \Sigma f_{Fy} = f_{Fx} \cos \delta - f_{Fy} \sin \delta. \quad (10)$$

Given the vertical displacement of the C.G. z , and the pitch angle θ , and their rates of change, the normal load of each wheel is given by

$$f_{Fz} = mg \frac{\ell_R}{\ell_F + \ell_R} - K_F \Delta z_F - C_F \Delta \dot{z}_F, \quad (11)$$

$$f_{Rz} = mg \frac{\ell_F}{\ell_F + \ell_R} - K_R \Delta z_R - C_R \Delta \dot{z}_R, \quad (12)$$

where

$$\begin{aligned} \Delta z_R &= z + \ell_R \sin \theta, & \Delta z_F &= z - \ell_F \sin \theta, \\ \Delta \dot{z}_R &= \dot{z} + \ell_R \cos \theta \dot{\theta}, & \Delta \dot{z}_F &= \dot{z} - \ell_F \cos \theta \dot{\theta}. \end{aligned}$$

III. OPTIMAL CONTROL FORMULATION

In this section we formulate the problems of minimum time and maximum exit velocity through a corner of a vehicle as problems in optimal control. We consider a 90 deg corner, which the vehicle has to negotiate (Fig. 3). The system dynamics have been derived in the previous sections and are given by equations (1)-(??), (8) and (9). In order to formulate the optimal control problem, it is necessary to define the cost function to be optimized, and specify all state/control constraints and boundary conditions.

A. Cost Function

For the time minimization problem the cost function is given by

$$J = t_f. \quad (13)$$

For the exit velocity maximization problem the cost function is given by

$$J = -\sqrt{\dot{x}_f^2 + \dot{y}_f^2}. \quad (14)$$

B. State and Control Constraints

The state constraint for the 90 deg corner is shown in Fig. 3 and can be described by the following inequality

$$8 \leq \sqrt{x^2 + y^2} \leq 10 \quad \text{when} \quad x \geq 0 \quad \text{and} \quad y \geq 0. \quad (15)$$

The state constraint above applies to the C.G. of the vehicle. Two straight segments of 5m each have been added before and after the corner so that the car enters the corner after travelling straight, and exits the corner in a posture that will lead again to straight travel.

The control inputs are the accelerating/braking torques T_F and T_R of each axle and the steering angle δ . In order to take into consideration the limited power that is provided by the engine, transmission and braking systems, as well as the physical limits of the steering mechanism, we choose the following control constraints

$$-1000 \text{ Nm} \leq T_i \leq 1000 \text{ Nm} \quad (i = F, R), \quad (16)$$

$$-0.7 \text{ rad} \leq \delta \leq 0.7 \text{ rad}. \quad (17)$$

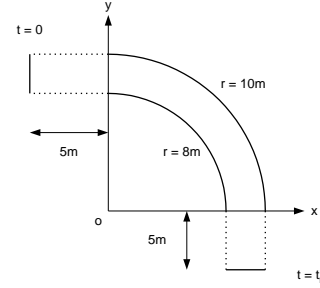


Fig. 3. State constraint for the 90° corner

C. Boundary Conditions

The boundary conditions are summarized in Table I. These conditions guarantee that the vehicle travels straight before and after the corner, i.e., there is zero lateral velocity, yaw velocity and slip angle β at $t = 0$ and $t = t_f$. The initial and final position of the car is within the width of the road. The final time and the longitudinal velocity at t_f are left free. The suspension states z , \dot{z} , θ and $\dot{\theta}$ initially take their equilibrium values and are left free at final time. The initial longitudinal velocity is fixed, in order to minimize the number of free variables and make convergence easier. In the case of time minimization we choose $\dot{x} = 10$ m/sec, while in the case of exit velocity we choose $\dot{x} = 8$ m/sec. In both cases we have chosen the highest values of initial velocities that allow convergence of the optimization algorithm. Initial values for ω_i ($i = F, R$), are such that zero slip is produced initially while the final values are left free.

TABLE I
BOUNDARY CONDITIONS

Position	Attitude	Velocities	Suspension
$x_0 = -5$	$\psi_0 = 0$	$\dot{y}_0 = 0$	$z_0 = 0$
$8 \leq y_0 \leq 10$	$\psi_f = -\frac{\pi}{2}$	$\dot{x}_f = 0$	$\dot{z}_0 = 0$
$8 \leq x_f \leq 10$		$\dot{\psi}_0 = 0$	$\theta_0 = 0$
$y_f = -5$		$\dot{\psi}_f = 0$	$\dot{\theta}_0 = 0$

D. Optimization Algorithm

The optimal control problem is solved numerically using EZOPT, a direct optimization software available by Analytical Mechanics Associates Inc., which uses collocation to transcribe an optimal control problem to a nonlinear programming problem. It provides a gateway to NPSOL, a nonlinear optimization program (for details see [10]). The optimization algorithm involves discretization of the independent variable (time). The control inputs are approximated with constant functions for each time interval. The user is required to provide the system's dynamics, the cost to be optimized, state constraints, boundary conditions and an initial guess for the optimal control inputs and states time history. The convergence of the algorithm depends on the complexity of the problem and the accuracy of the initial guess.

We have chosen time to be the independent variable resulting in an optimal control problem of free "final time". In [5], [6] and [7] time is replaced by travelled

distance as the independent variable resulting in a fixed “final time” optimal control problem, which is easier to converge numerically to a solution. However this change of variable results in a singularity when the vehicle travels with large slip angles. While such a scenario is never encountered in F1 racing, it is very common in rally-racing where drivers often drift through corners at large slip angles. This justifies the choice of the independent variable in this work.

IV. NUMERICAL OPTIMIZATION RESULTS

In this section we discuss the numerical solution (trajectory, states and control inputs) of the optimal cornering problem for minimum time of travel and maximum exit velocity. Two extreme cases for the vertical position of the C.G. are taken into consideration ($h = 1$ m and $h = 0$ m) for each case of the optimization cost in order to investigate the effects of the suspension dynamics and longitudinal load transfer. In the case $h = 0$ m the suspension dynamics are not included in the overall vehicle dynamics and no load transfer occurs. The longitudinal position of the C.G. is chosen to be slightly towards the rear of the vehicle, resulting in a slight over-steering (more agile but unstable configuration) vehicle. The tire friction capacity is equal along the longitudinal and lateral directions, i.e., the tire friction force lies within a friction circle.

A. Minimum Time Case

Figures 4, 5, 6 and 7 completely describe the optimal solution for the minimum time problem. Figure 4 shows the time histories of each state of the system provided directly from the optimization algorithm. Figure 5(i) shows the optimal control inputs. Figure 5(ii) shows the magnitude of the velocity vector versus time, the acceleration of the vehicle with respect to the inertial frame along the longitudinal body axis and the radius of the trajectory. The longitudinal acceleration along with the height of the center of gravity is the cause for the longitudinal normal load transfer; acceleration of the vehicle causes load transfer from the front axle to the rear (this may be verified by observing the longitudinal acceleration and normal load plots of Fig. 5(ii), (iii) and (iv)). The radius of trajectory is calculated using the formula for the centripetal force, $F_c = mv^2/R$.

In Fig. 6 we have the longitudinal, lateral and total friction coefficients of the front and rear tires (with a tire saturation level of 0.7), and finally in Fig. 5(iii) and (iv) we have the time history of the longitudinal and lateral components of the friction forces in the front and rear tires. Finally in Fig. 7 we present the trajectories for the optimal time problem, for both cases of $h = 1$ m and $h = 0$.

1) *Trajectory*: The trajectory in the case of time minimization (Fig. 5(ii) and 7) consists of a circular arc of (almost) constant radius ($0.5 \text{ sec} \leq t \leq 1.8 \text{ sec}$), through which the vehicle performs a steady-state cornering ($\dot{\psi} \approx 0$, $\dot{\delta} \approx 0$) as defined in [2] and [3], and two transients ($t \leq 0.5 \text{ sec}$ and $1.8 \text{ sec} \leq t$) since the boundary conditions enforce that the vehicle enters and exits the

corner travelling straight. The bigger the radius of the trajectory the higher is the velocity that the vehicle can drive through the corner for a given maximum centrifugal force (determined by the tire friction limits).

However, observing Figs 4 and 7 we notice that the vehicle does *not* enter or exit the corner at the limit of the state constraint. This means that there may exist a trajectory of bigger radius. This trajectory would allow the car to drive through the corner with higher speed, but the distance travelled would also be greater. Such a trajectory may not necessarily minimize time.

In conclusion, the optimal trajectory in the case of time minimization tends to a single circular arc with such a radius that compromises between the highest possible travel speed and the shortest distance travelled. No significant differences can be observed between the trajectory with $h = 1$ m and the one with $h = 0$ m (Fig. 7), and thus no conclusions about the role of suspension dynamics and load transfer may be derived taking into account only the shape of the trajectory.

2) *Control History and Response*: Figure 5 shows the control input history. We observe that the steering angle δ has initially a negative value, up to $t \approx 1$ sec. This creates immediately a lateral friction force on the front wheel (see Fig. 5(iii)). This initial lateral friction serves two purposes. The first is that it operates as a centrifugal force for the vehicle, and the second is that it initiates the yawing motion of the car. This yawing motion results in a lateral motion of the rear wheel of the vehicle; thus, a lateral slip and lateral friction (which contributes to the total centripetal force) is also generated at the rear wheel. We observe that the steering angle is gradually reduced, and actually at around $t = 2$ sec it changes its sign (“opposite lock”). This is done in order to decelerate the yawing motion and eventually eliminate it altogether by the time the car exits the corner. We observe that there is some overshoot about the desired final yaw angle and the steering angle changes again its sign at the end.

We also observe that the input torque of the rear wheel is initially ($t < 1$ sec) such that a braking friction force is generated in order to regulate the speed of the car to a value that makes it possible for the car to follow the optimal trajectory. Recall that the trajectory gradually increases its curvature and thus the maximum possible velocity through the trajectory is decreasing. The longitudinal slip of the front wheel generates an accelerating friction force which compensates for the braking component of the front wheel lateral friction force. The situation where the front wheel is accelerating while the rear wheel is braking is possible via a simultaneous use of handbrake and throttle. This is a standard maneuver performed by expert race drivers of off-road vehicles [9].

Notice from Fig. 6 that the total friction generated by the front tire is equal to the tire’s force capacity. In case the front tire is not saturated by lateral force, an accelerating longitudinal force is generated to make use of the total force capacity of the tire. As far as the friction generated by the rear tire, observing Fig. 6 we notice that it is also most of the times equal to its maximum.

Nonetheless, we observe that the friction of the rear tire is not maximum at $t \geq 2.25$ sec. Since the car is at the exit of the corner, one would expect that there should be maximum acceleration. However, at this point the front wheel is saturated with lateral friction in order to stop the yawing motion. More acceleration (which *is* available since the driven rear tire is not saturated) would require more effort from the front tire to stop the yawing motion; such an effort in this case is *not* available, however.

Although we were not able to distinguish any differences in the two trajectories in Fig. 7, it is clear from Fig. 5(ii) that the radius of the trajectory for $h = 0$ m is smaller from the one for $h = 1$ m except from the first 0.5 sec that the opposite holds. The magnitude of the velocity, again from Fig. 5(ii) is also in accordance to the difference in radius, since higher velocities are possible for higher values of trajectory radii. In fact, for the case of $h = 0$ m we observe an initial acceleration from the initial speed and then deceleration in the first 0.5 sec. From then on the velocity and trajectory radius are higher for the $h = 1$ m case.

In the $h = 1$ m case, where the suspension dynamics and load transfer effects are active, the initial acceleration is avoided because this would result in load transfer from the front axle to the rear axle, making the front wheel (which initiates cornering) produce less friction force. The front wheel is “more important” at the beginning of cornering, because it is the one initiating centripetal forces and yawing moments. The rear wheel becomes “more important” at the exit of the corner because it provides yaw damping. In both $h = 1$ m and $h = 0$ m cases we have deceleration until the apex of the corner end then acceleration towards the exit. In the $h = 1$ m case acceleration results in normal load transfer to the rear wheel, and thus greater yaw damping by the rear wheel, together with less effort from the front wheel to stop the yawing motion. In the $h = 0$ m case there is no change in the normal load distribution to front and rear axles. The front wheel is saturated with lateral friction in order to stop the yawing motion, which does not allow higher travel speed. The only way for the vehicle in the $h = 0$ m case to compensate for this loss of speed at the exit is to gain some time at the entry (first 0.5 sec).

The fact that in the $h = 1$ m case the trajectory radius is higher after $t = 0.5$ sec results in less steering angle δ as we can see in Fig. 5 (i). We also observe more torque applied to the rear wheel and less to the front toward the exit of the corner. This is related to the fact that the load transfer makes the rear wheel “heavier” (and respectively the front wheel “lighter”), implying that higher torque is needed to accelerate it.

B. Maximum Exit Velocity Case

In this section we investigate the maximum exit velocity solution. For brevity we omit the suspension dynamics and only consider the $h = 0$ m case. In Fig. 8 we present the optimal control inputs and the trajectory of the vehicle for the new optimization cost. The exit velocity is about 13 m/sec, while in the minimum time case that

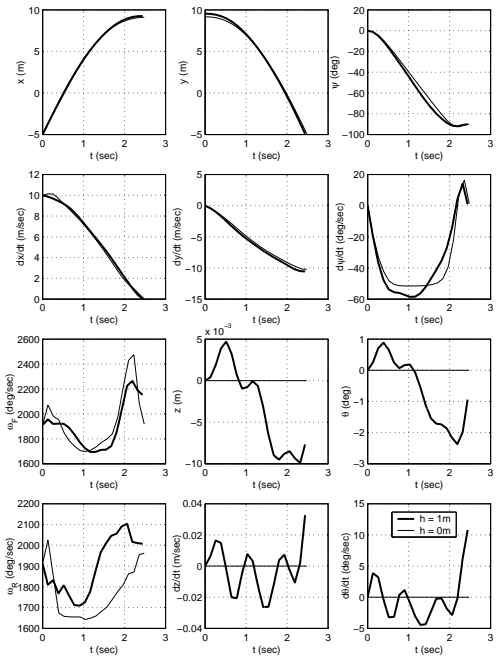


Fig. 4. Minimum time solution, states

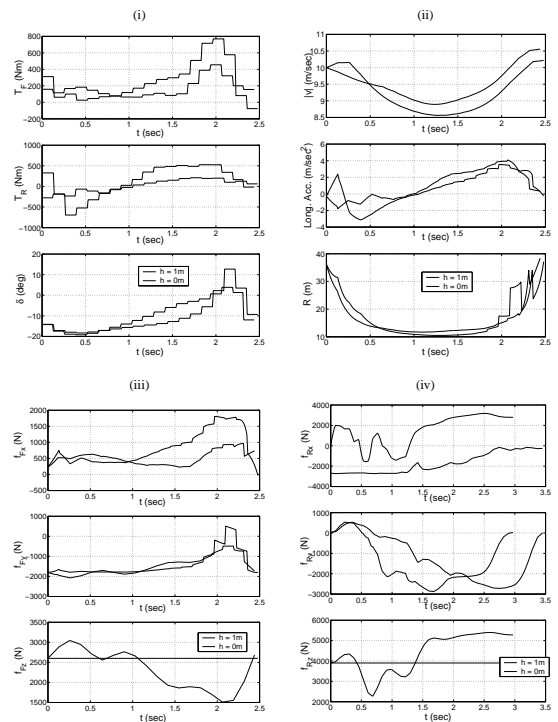


Fig. 5. Minimum time solution, inputs, absolute velocity, longitudinal acceleration, trajectory radius and wheel forces

was 11.5 m/sec. The travel time is now 3.4 sec while in the minimum time case that was 2.49 sec.

The trajectory in the case of exit velocity maximization is different and more complex compared to the case of time minimization. Since time is not minimized, the distance travelled does not need to be minimal, allowing the trajectory to reach the outer boundary of the corner and then aim at the inner boundary close to the exit. This results in a maximum radius trajectory at the exit of the

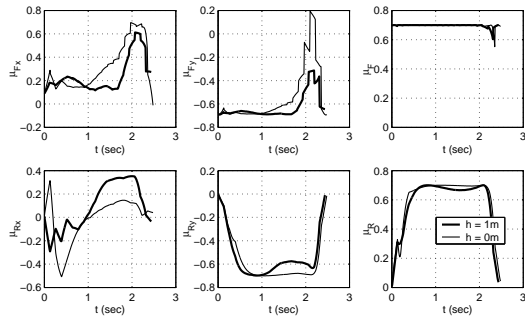


Fig. 6. Minimum time solution, friction coefficients

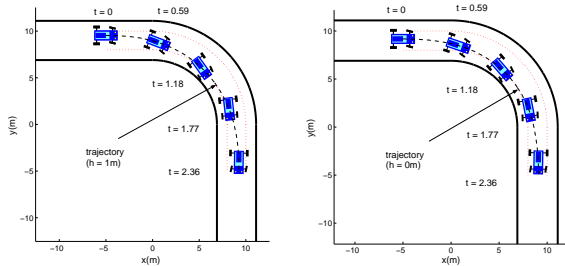


Fig. 7. Minimum time solution, trajectories

corner. As a result, the vehicle can accelerate while still in the corner, thus maximizing its exit velocity.

We also notice a pattern of an initially short turn to the opposite direction of the corner (call it the transitional part of the trajectory). Here, the car does *not* travel initially along the outer boundary of the corner. Instead, the initial position is clearly inside the road boundary and a turn to the opposite direction of the corner is necessary for the vehicle to reach the outer edge of the road. This allows yaw acceleration to develop and make the transit to the last part of the trajectory (the part of big radius) smoother, without the need of a large deceleration. In other words, if the car was travelling straight along the outer edge of the road until the point that the final segment of the trajectory starts, a sharp turn would be necessary, as well as a hard deceleration in order to negotiate the impeding sharp turn.

Finally, we present the results of yet another optimization scenario shown in Fig. 9, which corresponds to the exit velocity maximization case ($h = 0$ m) with a different vehicle configuration. For this scenario we have chosen a neutral-steering weight balance (50% on the front axle and 50% on the rear). We have also chosen reduced lateral

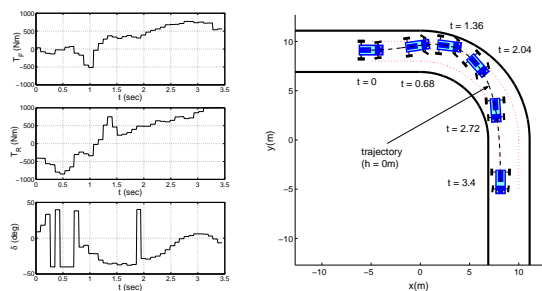


Fig. 8. Optimal control inputs and trajectory for the maximum exit velocity.

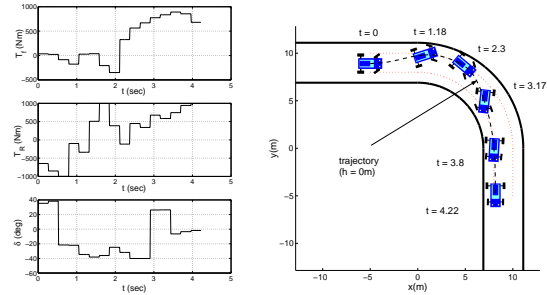


Fig. 9. Drifting through a corner.

tire friction incorporating a friction ellipse, which is more realistic than the friction circle ([3]). The new weight balance configuration (along with equal tire characteristics for front and rear axles) implies that saturation of the front and rear wheels with lateral friction will occur simultaneously [3]. Thus, large vehicle slip angles are not accompanied by uncontrollable oversteer or understeer, where path following capacity is lost, and result in a stable vehicle drift (see Fig. 9, for $2.3 \text{ sec} \leq t \leq 3.8 \text{ sec}$).

V. CONCLUSIONS

In this paper we have investigated how one may reproduce race driving behaviors using numerical optimization techniques. All types of car races are not the same, and driving through each segment of the circuit in the shortest time is not always the best strategy. Any motor-sports fun can distinguish between the smooth trajectories and small slip angles used in F1 driving in contrast to the more complex trajectories and drifting techniques in rally-race driving. We have shown that both behaviors may be reproduced by considering an optimization scheme, as long as the cost function is chosen in accordance to the specific needs of each type of race. A half-car model with suspension dynamics was used to investigate the effects of longitudinal normal load transfer in the limit operation of the vehicle.

REFERENCES

- [1] J. Wong, *Theory of Ground Vehicles*. New York: John Wiley and Sons, Inc., 1978.
- [2] T. Gillespie, *Fundamentals of Vehicle Dynamics*. Warrendale PA USA: Society of Automotive Engineers (SAE) International, 1992.
- [3] W. Milliken and D. Milliken, *Race Car Vehicle Dynamics*. Warrendale PA USA: Society of Automotive Engineers (SAE) International, 1995.
- [4] T. Fujioka and M. Kato, "Numerical analysis of minimum-time cornering," in *Proceedings of AVEC 1994*, November 24-28 1994. Tsukuba, Japan.
- [5] J. Hendriks, T. Meijlink, and R. Kriens, "Application of optimal control theory to inverse simulation of car handling," *Vehicle System Dynamics*, vol. 26, pp. 449-461, 1996.
- [6] D. Casanova, R. S. Sharp, and P. Symonds, "Minimum time manoeuvring: The significance of yaw inertia," *Vehicle System Dynamics*, vol. 34, pp. 77-115, 2000.
- [7] D. Casanova, R. S. Sharp, and P. Symonds, "On minimum time optimisation of formula one cars: The influence of vehicle mass," in *Proceedings of AVEC 2000*, August 22-24 2000. Ann-Arbor, MI.
- [8] E. Bakker, L. Nyborg, and H. Pacejka, "Tyre modelling for use in vehicle dynamics studies," *SAE paper # 870421*, 1987.
- [9] "<http://www.modernracer.com/tips/tips.html>."
- [10] P. Gill, W. Murray, M. Saunders, and M. Wright, *User's Guide for NPSOL (version 4.0)*. Dept. of Operations Research, Stanford University, CA, 1986. Report SOL 86-2.